Title

Soluble epoxide hydrolase inhibition enhances production of specialized pro-resolving lipid mediator and promotes macrophage plasticity

Journal

British Journal of Pharmacology, 180(12)

ISSN

0007-1188

Authors

Abdalla, Henrique B

Alvarez, Carla

Wu, Yu-Chiao

et al.

Publication Date

2023-06-01

DOI

10.1111/bph.16009

Peer reviewed

HHS Public Access

Author manuscript

Br J Pharmacol. Author manuscript; available in PMC 2024 June 01.

Published in final edited form as:

Br J Pharmacol. 2023 June ; 180(12): 1597–1615. doi:10.1111/bph.16009.

Soluble epoxide hydrolase inhibition enhances Specialized Pro-resolving Lipid Mediator production and promotes macrophage plasticity

Henrique B. Abdalla[a,b,1], **Carla Alvarez**[a,1], **Yu-Chiao Wu**[a,c], **Paola Rojas**[a], **Bruce D Hammock**[d], **Krishna R. Maddipati**[e], **Carlos Antonio Trindade-da-Silva**[b], **Mariana Q. S. Soares**[b], **Juliana T. Clemente-Napimoga**[b], **Alpdogan Kantarci**[a], **Marcelo H. Napimoga**[b,1,*], **Thomas E. Van Dyke**[a,f,1,*]

[a]Department of Applied Oral Sciences, The Forsyth Institute, Cambridge, MA, USA.

[b]Laboratory of Neuroimmune Interface of Pain Research, Faculdade São Leopoldo Mandic, Instituto de Pesquisa São Leopoldo Mandic, Campinas, Brazil.

[c]Harvard School of Dental Medicine, Boston, MA, USA.

[d]Department of Entomology and UCD Comprehensive Cancer Center, University of California, Davis, California, USA.

[e]Department of Pathology, Wayne State University, Detroit, MI, USA.

[f]Department of Oral Medicine, Infection, and Immunity, Faculty of Medicine, Harvard University, Boston, MA, USA.

Abstract

Background and Purpose: Epoxyeicosatrienoic acids (EETs) and other epoxy fatty acids (EpFA) are lipid mediators that are rapidly inactivated by soluble epoxide hydrolase. Uncontrolled and chronic inflammatory disorders fail to sufficiently activate endogenous regulatory pathways, including the production of specialized pro-resolving mediators (SPMs). Here, we addressed the relationship between SPMs and the EET/sEH axis and explored the impact of sEH inhibition on resolving macrophage phenotype.

* To whom correspondence may be addressed. **Corresponding author:** Dr. Thomas E. Van Dyke, Clinical and Translational Research, Forsyth Institute, Cambridge, MA 02142. tvandyke@forsyth.org.

[1]Equally contributed to this work

Author contributions

H.B.A., M.H.N., and T.E.V.D. conceived and designed the study. H.B.A., C.R.A., Y.W., P.R., C.A.T.S. performed the in vivo and in vitro experiments. K.R.M. performed the LC-MS/MS analysis. M.Q.S.S. analyzed the μCT data. T.E.V.D., A.K., B.D.H., provided and generated reagents. The data collected was interpreted by H.B.A., C.R.A., T.E.V.D., A.K., K.R.M., J.T.C.N, B.D.H., and M.H.N. H.B.A. wrote the original manuscript. T.E.V.D and M.H.N. revised the manuscript. All contributing authors have agreed to the submission of this manuscript for publication.

Conflict of Interest

Dr. Van Dyke is an inventor of several granted and pending licensed and unlicensed patents awarded to the Forsyth Institute that are subject to consulting fees and royalty payments. B.D. Hammock is inventor on a university of California patents for synthesis and application of sEH inhibitors for disease treatment. All other authors declare that they have no competing interests.

Declaration of Transparency and Scientific Rigour

The authors declare that this study follows to the principles for transparent reporting and scientific rigour of preclinical research as stated in the ***BJP*** guidelines for Design & Analysis, Immunoblotting and Immunochemistry, and Animal Experimentation, and as recommended by funding agencies, publishers, and other organizations engaged with supporting research.

Experimental Approach: Mice were treated with an sEH inhibitor, EETs, or sEH inhibitor + EETs (combination) before ligature placement to induce experimental periodontitis. Using RT-qPCR, gingival samples were used to examine SPM receptors and osteolytic and inflammatory biomarkers. Maxillary alveolar bone loss was quantified by μCT and methylene blue stain. Salivary metabololipidomics were carried out to analyze SPM levels. Gingival macrophage phenotype plasticity was determined by RT-qPCR and Flow Cytometry. Bone marrow-derived macrophages were isolated to investigate the impact of sEH inhibition on macrophage polarization and SPM production.

Key Results: We report that pharmacological inhibition of sEH suppresses bone resorption and the inflammatory cytokine storm in experimental periodontitis. Lipidomic analysis revealed that sEH inhibition augments levels of LXA4, RvE1, RvE2, and 4-HDoHE, concomitant with up-regulation of LTB4R1, CMKLR1/ChemR23, and ALX/FPR2 SPM receptors. Notably, there is an impact on gingival macrophage plasticity favoring an inflammation resolving phenotype with sEH inhibition. In bone marrow-derived macrophages (BMDMs), sEH inhibition reduces inflammatory macrophage activation, and resolving macrophages are triggered to produce SPMs.

Conclusion and Implications: Pharmacological sEH inhibition positively impacts SPM synthesis associated with resolving macrophages, suggesting a potential target to control osteolytic inflammatory disorders.

Keywords

Soluble epoxide hydrolase inhibition; Specialized pro-resolving mediators (SPMs); inflammation; periodontal disease; macrophage

1. INTRODUCTION

Periodontitis is a chronic osteolytic inflammatory disease that is the sixth most common worldwide, representing a significant socioeconomic burden (Hajishengallis & Chavakis, 2021; Lamont & Hajishengallis, 2015). The pathogenesis is complex and multifaceted, encompassing the host immune response and oral microbiome dysbiosis, leading to a hyperinflammatory state, destruction of soft and hard tissues, and ultimately tooth loss (Alvarez et al., 2019; Van Dyke & Sima, 2020). It was assumed that periodontal disease pathogenesis was microbial-driven as a principal component of disease progression for years. However, a shift in the understanding of periodontitis etiology and pathogenesis emerged in the early 2000s with the realization that while oral biofilms on the teeth are the initial etiologic driver of inflammation, it is uncontrolled inflammation that drives pathogenesis ultimately changes the biofilm composition creating dysbiosis, increasing inflammation and destruction of tissues (Van Dyke, Bartold & Reynolds, 2020; Balta et al., 2021).

The reasons for excess inflammation in periodontitis have long been though to center on excess production of proinflammatory mediators. More recently, the focus has shifted to a failure of regulatory pathways responsible for controlling inflammation. Indeed, in periodontitis, we now realize that the balance between pro-inflammatory and pro-resolution of inflammation pathways is the keystone for determining health or disease (Balta et

al., 2021; Van Dyke, 2020b). This is also likely true for associated chronic conditions such as arthritis, cancer, diabetes, and inflammatory bowel disease (Fishbein et al., 2021; Serhan & Savill, 2005). In health, inflammation is self-perpetuating, but also self-limiting, traditionally split into initiation and resolution stages (Serhan & Levy, 2018). The resolution of inflammation is a highly coordinated and active process, intended to rebuild tissue homeostasis, stem excess leukocyte infiltration, stimulate local immune cells (e.g., macrophages), clear cellular debris, and regulate eicosanoid and cytokine synthesis (Panigrahy et al., 2021). In the resolution phase, aside from the classical lipid mediators (the eicosanoids prostaglandins, and leukotrienes), which display a fundamental role in leukocyte trafficking, a novel class of pro-resolving lipid mediators (LMs), called, stand out as essential lipids for inflammation termination. The SPM superfamily comprises polyunsaturated fatty acid (PUFA)-derived metabolites, including the lipoxins (LXs; arachidonic acid-derived), resolvin E-series (RvEs; eicosapentaenoic acid (EPA)-derived), resolvin D-series (RvDs; docosahexaenoic acid (DHA)-derived), and others, such as maresins and protectins (Panigrahy et al., 2021).

Eicosanoids are a group of lipid mediators produced by metabolism of arachidonic acid (AA) by the cytochrome P450, cyclooxygenases and lipoxygenases, that yield EpFA, prostaglandins and thromboxanes, and leukotrienes, respectively (Serhan, 2014; Wang & Dubois, 2010). These eicosanoids are commonly recognized as pro-inflammatory lipid mediators, causing the initiation of cytokine storm, inflammasome activation, and endoplasmic reticulum (ER) stress response (Hammock et al., 2020). Conversely, epoxyeicosatrienoic acids from AA (EETs; 5,6-EET, 8,9-EET, 11,12-EET, and 14,15-EET) as well as epoxides of other long chain poly unsaturated fatty acid (EpFA), are eicosanoids derived from AA metabolism by a third enzymatic pathway called cytochrome P450 (CYP450) (Zeldin, 2001). EETs are important bioactive lipids with potent modulatory actions in inflammation. However, EETs are short-lived, due to their quick conversion into dihydroxyeicosatrienoic acids (DHETs) in the presence of soluble epoxide hydrolase (sEH) and to a lesser extent the microsomal epoxide hydrolase (mEH), losing their biological function in the control of inflammation (Hammock et al., 2020). By knocking out sEH or inhibiting it pharmacologically, therapeutic efficacy was demonstrated in several inflammatory diseases, such as rheumatoid arthritis (Trindade-da-Silva et al., 2020), periodontitis (Trindade-da-Silva et al., 2017; Napimoga et al., 2018), ovarian and hepatocellular cancer (Gartung et al., 2019; Fishbein et al., 2020), cardiovascular disease (McReynolds et al., 2020), and others. In periodontitis and knee arthritis, sEH levels are significantly increased (Trindade-da-Silva et al., 2017; Trindade-da-Silva et al., 2020). Additionally, pharmacological sEH inhibition enhances 5-epi-LXA_4 levels in the blood of patients with severe asthma (Ono et al., 2014).

Here, we demonstrate that pharmacological inhibition of sEH prevents the bone resorption in experimental periodontitis. We further sought to determine whether pharmacological sEH inhibition stimulates SPM production, and our lipidomic data demonstrate that levels of LXA_4, RvE1, RvE2, and 4-hydroxy docosahexaenoic acid (4-HDoHE) are enhanced in saliva with sEH inhibition. The expression of the SPM receptors LTB4R1, CMKLR1/ChemR23, and ALX/FPR2 was consistently upregulated by pharmacological sEH inhibition. Importantly, the inflammatory cytokine storm is blocked, and gingival macrophage plasticity

is impacted by pharmacological sEH inhibition favoring a resolving macrophage phenotype. *In vitro*, EETs and sEH inhibition diminished inflammatory macrophage activation, whereas resolving macrophages were triggered. Collectively, our findings uncover for the first time an interaction between sEH inhibition and SPM production that promotes gingival resolving macrophage phenotype, demonstrating the therapeutic potential of sEH inhibitors as immunoresolvents that may play a role in the treatment of osteolytic inflammatory diseases.

2. METHODS

2.1. Reagents.

We used the sEH inhibitor 1-(1-propanoylpiperidin-4-yl)-3-[4-(trifluoromethoxy)phenyl]urea (TPPU), which was synthesized at the Department of Entomology and Nematology, University of California-Davis (USA) as previously published (Rose et al., 2010). Dose titration was performed to obtain a working dosage for further experiments. TPPU was weighed and dissolved in a glass container in polyethylene glycol 400 (PEG400; Sigma). The glass container was sealed with Parafilm M (Sigma) tape and submerged in a sonicator chamber until complete TPPU dissolution. Likewise, the mixture of EET regioisomers (5,6-EET, 8,9-EET, 11,12-EET, and 14,15-EET) was synthesized at the Department of Entomology and Nematology, University of California-Davis (USA), using procedures published previously (Morisseau et al., 2010). The EET stock solution (10 mM diluted in DMSO) was kept at −80°C. EETs were thawed and dissolved in PEG400 at a 1 μg/kg dose for each experiment. For saliva collection, pilocarpine (Sigma-Aldrich) and isoproterenol (Sigma-Aldrich) were used to stimulate saliva secretion in mice. Both compounds were diluted in sterile saline and used once.

2.2. Animals.

8-week-old male C57BL/6 mice were purchased from Jackson Laboratory and kept in a pathogen-free environment, at 24° ± 0.5°C, with a light/dark cycle of 12:12 hours, with food and water *ad libitum*. Animals were randomly allocated in conventional plastic cages containing aspen wood as bedding material and environmental enrichment. Five animals were assigned to each cage. The block method was used for randomization, and investigators were blinded to the treatments. All experiments were approved by the Institutional Animal Care and Use Committee of the Forsyth Institute (#17–020) and are reported in compliance with the ARRIVE guidelines (Kilkenny et al., 2010).

2.3. Periodontitis model and treatments.

Animals were initially anesthetized with a mixture of ketamine (10ml/kg) and xylazine (0.86 mg/ml) in sterile saline, intraperitoneally. Mice were then placed in an animal-holding structure, and 6.0-silk ligatures were tied around the second molars in the upper jaws for 14 days (Marchesan et al., 2018). Oral treatment was initiated two hours before ligature placement and continued daily until the protocol ended. TPPU dose titration of 10 ng/kg, 100 ng/kg, 1 mg/kg, 10 mg/kg, and 20 mg/kg was performed. EET-mix was administered in a unique dose of 1 μg/kg. In addition, animals were treated with EET-mix, or the combination of sEH inhibitor and EET-mix. As a control, animals received vehicle treatment

(PEG400). On day 14, mice were euthanized, and the presence of ligature was verified before sample collection (gingival tissue and maxillae).

2.4. Quantification of Alveolar Bone Loss and Micro-computed microtomography (μCT).

Dermestid beetles were used to remove soft tissues from maxillary bones for a week. The maxillae were then kept in 10% hydrogen peroxide overnight. The samples were washed in running tap water and dried the day after. Samples were stained with methylene blue. An Axio Observer A1 microscope (ZEISS) was used to capture the images at 0.63 × 10 magnification. Bone loss was quantified using Fiji software (ImageJ) as the area from the alveolar bone crest to the cementoenamel junction (CEJ) on the palatal side of each tooth.

Further, samples were scanned with μCT40.scanco (Medical AG, Bassersdorf, Switzerland) at scanning parameters of 70kV, 114 μA and 8.0μm3 voxel size. Images were reconstructed and exported as Digital Imaging and Communications in Medicine (DICOM) files for analysis. Three-dimensional morphometric analysis was performed with CT-Analyzer software® (Bruker, Belgium). A volume of interest (VOI), including the entire alveolar bone surrounding the roots of the second molar, was individually selected for all samples. The bone within the VOI was segmented using a global automatic thresholding algorithm. Bone Volume (BV) was calculated in mm3.

2.5. Quantitative real-time PCR (qPCR):

Gingival tissue surrounding the upper molars was gently removed using a scalpel blade (#15C) under a microscope and conditioned in RNAlater solution (Life Technologies). Glassware was used to grind and homogenize the samples in 300 μL of RLT lysis buffer (Qiagen). Then samples were further homogenized using QIAshredder columns (Qiagen), according to the manufacturer's recommendations. Total RNA was isolated from the homogenized gingiva using the RNeasy Mini Kit (Qiagen), following the kit instructions. A total of 1 μg of RNA was used for cDNA synthesis using the reverse transcription kit (SuperScript III, Invitrogen). The cDNA amplification (50 ng) was performed using TaqMan™ Fast Advanced Master Mix (Thermo Fisher). All TaqMan probes of genes quantified and investigated in this study were purchased from Thermo Fisher (Supplementary Table 1). The sEH gene quantification was carried out using the following sequence: Ephx2, F – 5'-GGCACTGCCTAGAGACTTCCT-3'/ R – 5'-CAGGTAGATTGGCTCCACAGG-3'. The reaction product was quantified with the Relative Quantification tool, using β-actin as the reference gene. The data are presented as a fold-change of relative quantity using the $2^{-\Delta\Delta Ct}$ method.

2.6. Flow Cytometry:

Gingival tissue surrounding the upper molars of mice was removed and placed in a falcon tube containing RPMI-1640 + 1% penicillin-streptomycin (Sigma). Samples were then treated with a solution with 0.15 μg/ml DNase I (GIBCO) + 3.2 mg/ml Collagenase Type IV (GIBCO) (Collagenase-DNase media) in 500 μl of RPMI-1640 + 1% penicillin-streptomycin in a 6-cm culture dish. Samples were then chopped with a sterile blade (#15). All sample fragments were collected in a 15 ml tube containing 4 ml Collagenase-DNase media and maintained in a water bath at 37°C for 1h. Fifty μl of 0.5M EDTA were

added during the last 5 min of incubation. Subsequently, samples were centrifuged at 1200 rpm for 10 min, and the supernatant was discarded. The remaining fragments were crushed onto a 70-μm cell strainer. The cells were filtered by rinsing the cell strainer constantly with RPMI-1640 + 1% penicillin-streptomycin + 0.15 μg/ml DNase I. The final cell suspension was centrifuged at 400g for 10 min; the supernatant was discarded, and the cells were re-suspended in 200 μl of PBS +5% fetal-bovine serum (FBS). Cells were counted (assessed by Trypan blue stain using a hemocytometer) and stained using the LIVE/DEAD Fixable Yellow Stain kit (Invitrogen) according to the manufacturer's instructions. Fc receptors were then blocked by TruStain FcX Antibody (Biolegend) according to the manufacturer's instructions. Extracellular staining was performed in PBS containing 5% FBS, using the following antibodies (Biolegend) for 30 min at 4°C in the dark: anti-I-A/I-E (M5/114.15.2), -CD45 (30-F11), -CD206 (C068C2), -CD64 (X54–5/7.1), -CD11b (M1/70), -CD11c (N418), -CD86 (GL-1), -CD80 (I6–10A1) and -Ly6C (HK14). As explained below, in vitro differentiated macrophages were recovered from culture plates, washed two times with PBS, and then stained as detailed above.

All samples were analyzed on an Attune™ NxT acoustic focusing cytometer (Invitrogen). To set the flow cytometry compensation, the AbC™ Total Antibody Compensation Bead Kit (Thermo Fisher Scientific) was used according to the manufacturer's instructions. The multiparametric data analysis was performed using FlowJo software v10.7.1 (CA, USA).

2.7. LM-SPM metabololipidomics:

For saliva collection, 100 μl of pilocarpine (1 mg/ml) and isoproterenol (2 mg/ml) were intraperitoneally injected to stimulate saliva secretion on the sample collection day (14th day). Saliva was collected continuously with a micropipette from the oral cavity for 5 min starting one minute after the stimulant administration. Saliva samples were stored in a −80 °C freezer until processing and analysis. LM-SPM metabololipidomics was carried out at the Lipidomics Core Facility, Wayne State University (Detroit, MI, USA), for quantitative analysis of SPM levels and other LMs (Ferguson et al., 2020; for detailed information). Protein concentration was determined by BCA Assay to normalize the LM data.

2.8. Bone marrow-derived macrophage (BMDM) cell culture:

Femora and tibiae of C57BL/6 mice were collected. Bone marrow cells were extracted and cultured for seven days in IMDM medium (Sigma), supplemented with 20% FBS (Sigma), penicillin (100 U/ml), amphotericin B (2 μg/mL) and 10ng/ml M-CSF, at 37°C in a 5% CO2 atmosphere (Ying et al., 2013). Cell viability was estimated by MTT assay, where the metabolism of the MTT tetrazolium salt into MTT formazan is directly proportional to the number of viable cells (Gerlier & Thomasset 1986). The BMDM cells were seeded at the density of 2.5 $\times 10^6$ cells for flow cytometry in a 24-well plate and 5×10^6 cells for RNA extraction in a 6-well plate. After 7 days of differentiation, the medium was changed for M1 activation (100ng/ml LPS; for 24 hours) or M2 activation (10ng/ml IL-4 and 10ng/ml IL-13; for 48 hours). The cells were treated with sEH inhibitor (TPPU) at 10, 100, or 200 μM/ml; and EET-mix at 0.1, 1, or 10 μM/ml. For M1 macrophages, cells were treated for 24 hours; for M2 macrophages, cells were treated for 48 hours. All cells were treated once.

2.9. Enzyme-Linked Immunosorbent Assay (ELISA):

Cell supernatants were collected and stored at −80 °C until molecular analysis. The levels of Lipoxin A4 (LXA4; Cayman Chemical, #90410) and Maresin 1 (MaR1; Cayman Chemical, #501150) were quantified by Enzyme-linked immunosorbent assay (ELISA). The assays were performed according to the manufacturer's recommendations.

2.10. Statistical analysis:

Data were analyzed by two-way analysis of variance (ANOVA) followed by Tukey's post hoc test for multiple comparisons using GraphPad 9.2. The metabolomic analysis was performed using the integrated web-based platform MetaboAnalyst (Xia & Wishart, 2011). Flow Cytometry data were analyzed applying a dimensionality reduction with the t-Distributed Stochastic Neighbor Embedding (tSNE) algorithm. All data are presented as mean ± SEM. A P-value lower than 0.05 was considered significant. The data and statistical analysis comply with the recommendations of the British Journal of Pharmacology on experimental design and analysis in pharmacology.

2.11. Nomenclature of Targets and Ligands

Key protein targets and ligands in this article are hyperlinked to corresponding entries in http://www.guidetopharmacology.org, and are permanently archived in the Concise Guide to PHARMACOLOGY 2021/22 (Bäck et al., 2020; Alexander, Christopoulos et al., 2021; Alexander, Fabbro et al., 2021; Alexander, Doherty et al., 2019).

3. RESULTS

3.1. sEH inhibition prevents bone loss and thwarts osteolytic mediator expression.

Here, we used ligature-induced periodontitis, which allows the natural formation of microbiome dysbiosis instead of inoculating an exogenous pathogen. We performed a dose titration of the sEH inhibitor to establish the most efficacious dose. The experimental design is summarized in Figure 1A. Pharmacological inhibition of sEH significantly prevented the alveolar bone loss in a dose-dependent manner in ligature-induced periodontitis ($P<0.05$; Figure 1B). Starting from 100 ng/kg, bone loss prevention is statistically significant; however, the first molar area still had bone defects at 100 ng/kg and 1 mg/kg, as observed in the representative images (Figure 1D). In this regard, we fixed the 10 mg/kg as an efficient and safe dosage for further experiments. Since pharmacological sEH inhibition has the function to improve endogenous EETs bioavailability (Inceoglu et al.,2007), we further assessed whether treatment with EETs solely could prevent alveolar bone loss. As expected, the treatment with EETs did not impact disease progression compared to non-treated animals ($P>0.05$, Figure 1C), presumably because the exogenous EETs delivered were metabolized rapidly by the endogenous sEH. We further investigated whether the combination of pharmacological sEH inhibition and EETs could improve the outcomes in bone resorption prevention (Figure 1C); the combination did not improve the outcome observed with pharmacological sEH inhibition, although it blocked bone resorption ($P<0.05$; Figure 1C). The representative images for each group and the area quantified are shown in Figure 1D. Subsequently, we analyzed bone volume by μCT surrounding the second

molar, where the ligature was placed (region of interest; Figure E). Representative μCT-3D reconstruction images of vestibular maxillary molars are shown in Figure 1F. The scanned maxillae revealed that pharmacological sEH inhibition conserves alveolar bone and crest volume compared to non-treated animals ($P<0.05$; Figure 1G). On the other hand, when animals were treated with the combination, no statistical changes were found compared to non-treated animals, even though a trend was observed ($P>0.05$; Figure 1G).

We then examined the expression of osteolysis hallmarks of periodontal disease that characterize the disease phenotype (Figure 1H – L). Consistent with bone resorption analysis, gingival mRNA expression of interleukin (IL) 17A was downregulated with pharmacological sEH inhibition and the combination with EETs ($P<0.05$; Figure 1I). Although EETs did not prevent bone resorption, a clear impact on IL-17A expression, a well-known inflammatory cytokine that activates osteoclast activity, was found ($P<0.05$; Figure 1I). The expression of RANKL (receptor activator of nuclear factor-kappa beta ligand) was also mitigated by sEH inhibition and the combination ($P<0.05$; Figure 1J), but not by EETs alone ($P>0.05$; Figure 1J). OPG (osteoprotegerin) levels did not show statistical differences between the non-treated animals and the treated groups ($P>0.05$; Figure 1K). Nevertheless, when the ratio of RANKL/OPG is examined, the combination presented the lowest balance, while the periodontal disease group and EETs exhibited the highest proportions ($P<0.05$; Figure 1L). Taken together, these findings showed that pharmacological sEH inhibition prevented bone resorption that is associated with a downregulation of gene expression of osteolytic factors.

3.2. Resolvin E-series and LXA_4 are enhanced in saliva and gingival SPM receptors are overexpressed.

The CYP450 metabolic lipid pathway, broadly synthesizes epoxy fatty acids from PUFA, lipid molecules with homeostatic functions (Hildreth et al., 2020). The SPMs consist of omega-3 polyunsaturated fatty acid-derived molecules, like resolvins and protectins, and arachidonic acid-derived molecules, such as lipoxins. sEH converts EpFAs from the CYP450 metabolism pathway to their diols (Schmelzer et al., 2005; Panigrahy et al., 2020). However, it is unexplored whether inhibition of epoxide hydrolysis also affects SPM levels and their receptors. We hypothesized that by inhibiting sEH activity, “communication” between the homeostatic and pro-resolution lipid biosynthetic pathways would enhance SPM production. Indeed, for the first time, we show that pharmacological inhibition of sEH impacts the SPM lipid profile and synthesis in saliva compared with periodontitis-induced animals (Figure 2). Principal component analysis (PCA) revealed that the lipid profiles are predominantly distinct from each other in two-dimensional (Figure 2A) and three-dimensional PCA (Figure 2B). In particular, the baseline (no disease) group forms clusters in the opposite direction of the periodontitis-induced animals; the groups treated with sEH inhibitor and treated with the combination fall between them (Figure 2A – B). Heatmap and cluster analyses were performed to investigate which mediators were most relevant among all mediators analyzed. Pharmacological inhibition of sEH significantly stimulates the release of bioactive lipid mediators (Figure 2C). Notably, 4 out of 50 LM-SPMs were highly distinguished (Figure 2D, E, F, and I). Individually, pharmacological sEH inhibition and the combination with EETs significantly stimulates the release of RvE1 ($P<0.05$; Figure

2D), RvE2 ($P<0.05$; Figure 2E), 4-HDoHE ($P<0.05$; Figure 2F), and LXA_4 ($P<0.05$; Figure 2I). Leukotriene B_4 (LTB_4) is a pro-inflammatory lipid mediator associated with bacterial infections, characteristic of periodontal disease. Although the sEH inhibitor and the combination group do not inhibit LTB_4 biosynthesis ($P>0.05$; Figure 2H), metabolism of LTB_4 to 20-hydroxy LTB_4 ($P<0.05$; Figure 2G), is amplified in both groups, suggesting the initiation of the inactivation of the inflammatory mediator. Finally, the combination group showed a significant increase in the levels of 4-HDoHE, which is a metabolite of the docosahexaenoic acid cascade (DHA), and an intermediate in the biosynthesis of SPMs ($P<0.05$; Figure 2F). Overall, the pharmacological inhibition of the sEH not merely preserves the bioactive lipids from the CYP450 pathway in the AA cascade; it is also likely that the EPA and DHA metabolic pathways are also influenced, stimulating SPM production and consequently regulating uncontrolled and aggressive inflammation.

Gene expression of SPM receptors is consistent with these findings showing distinct patterns among the groups (Figure 3). PCA analysis reveals that the sEH inhibitor and the combination-treated groups had the same SPM receptor profile. In contrast, the group treated with EET-mix and the periodontitis group were the opposite (Figure 3A). Figure 3B shows the three-dimensional plots. Heatmap and cluster analyses were performed to investigate the most relevant receptors and demonstrated the similarity between groups (Figure 3C). The receptors related to E-series resolvins (Rv E-series), LTB_4R1, and CMKLR1/ChemR23, exhibited increased expression in gingiva in animals treated with sEH inhibitor and combination ($P < 0.05$; Figure 3D and E). Furthermore, the ALX/FPR2 receptor, which is activated by RvD1, RvD2, and LXA_4, exhibited increased gene expression in the combination-treated group ($P < 0.05$; Figure 3F), as did the GPR18 receptor ($P < 0.05$; Supplementary Figure 3E). Taken together, the results of metabololipidomics associated with the gene expression of SPM receptors suggest a relationship between the inhibition of sEH and the production of SPMs. Therefore, it is possible to suggest that one of the possible mechanisms behind the protective role of TPPU in immuno-inflammatory osteolytic diseases is through a lipid bioactive class switch from pro-inflammatory eicosanoids to pro-resolving lipid mediators, such as the EPA and DHA family, including the RvE1 and RvE2 and other SPMs.

3.3. Altered macrophage plasticity stimulated by blocking sEH in the gingiva

Macrophages are essential leukocytes that orchestrate the inflammatory process and host defense and are central to the reparative and resolution phase. In osteolytic disorders, resolving macrophages regulate bone cells and are characterized by different lipid mediator profiles, especially by upregulating LXA_4 levels and downregulating LTB_4 release (Viniegra et al., 2018; Dalli & Serhan, 2016). Taking this into account, we attempted to uncover whether the protective actions of pharmacological sEH inhibition on bone resorption and SPM production is associated with swift macrophage plasticity. Gingival macrophages were assessed by flow cytometry using different membrane markers, and target genes were used to investigate their phenotype (Figures 4 and 5). To analyze gingival macrophage polarity, we used t-SNE (t-stochastic neighbor embedding)-based methods and examined the behavior of 4 extracellular markers among the gingival Macs ($CD45^+/CD11b^+/CD64^+$ cells) (Figures 4A–B). To effectively identify the distinct cell subpopulations, the following

workflow was applied: **1)** data was cleaned by manually excluding doublets, debris, and dead cells; **2)** Samples were gated for CD45+ cells; **3)** samples were linked; **4)** the linked samples were dimensionally reduced (tSNE parameters); **5)** distinct cell populations were analyzed and phenotypes identified (Alvarez et al., 2021).

The percentage of total gingival leukocytes ($CD45^+$ cells) was increased in experimental periodontitis ($P<0.05$; Figures 4A and D), and the percentage of Macs did not change among the groups ($P>0.05$; Figures 4B and E). The frequency of $MHCII^+$ cells gated as macrophages in the periodontal disease group increased compared to baseline animals, and the inhibition of sEH induced reduction ($P<0.05$; Figure 4F). Although the percentages of $CD11c^+$ cells gated as Macs are increased in sEH inhibitor and combination groups ($P<0.05$; Supplementary Figure 4A), and $CD206^+$ cells gated as Macs are decreased in the same groups compared to baseline ($P<0.05$; Supplementary Figure 4A), $CD11c^+/CD206^+$ double-positive cells (indicated in the black squares in Figure 4C) were markedly upregulated in sEH inhibitor and combination groups ($P<0.05$; Figure 4G). Next, we examined the mRNA expression of several cytokines and macrophages markers in the gingiva (Figures 5A–G). Overall, experimental periodontitis led to the expression of inflammatory mediators, such as TNF-α ($P<0.05$; Supplementary Figure 4D), iNOS ($P<0.05$; Figure 5B), IL-12 ($P<0.05$; Figure 5C), and IL-1β ($P<0.05$; Figure 5D), and sEH inhibition reversed increased expression ($P<0.05$; Figures 5B–D). Also, sEH blockage amplified genes that are characteristic of M2 polarization, including Arg-1 (arginase-1) ($P<0.05$; Figure 5F), CD206/Mrc1 ($P<0.05$; Figure 5E), and Retnla/FIZZ1 ($P<0.05$; Figure 5G). These findings indicated that rather than polarizing macrophages, pharmacological sEH inhibition simultaneously stimulated a dynamic transcriptional reprogramming of inflammatory macrophages toward reparative macrophages.

3.4. Impact of sEH inhibition and EETs on macrophage polarity and LXA_4 and MaR1 release in BMDMs.

To confirm whether inhibiting sEH influenced macrophage plasticity, bone marrow-derived macrophages (BMDMs) were isolated from the femur and tibia of mice and cultured in a growth medium with macrophage polarizing factors. The experimental design is summarized in Figure 6A. Initially, a cell viability test was performed to select a safe and effective dose (Figure 6B). Pharmacological sEH inhibition at doses of 100 and 200 μM significantly decreased cell viability in both primed media, while EETs did not affect cell viability at any concentration ($P<0.05$; Figure 6B). Therefore, we fixed 10 μM of TPPU and EETs for the experiments. To endorse the involvement of sEH inhibition and the macrophage plasticity, we further examined distinct membrane markers for M1 and M2 macrophages using the same t-SNE strategy with flow cytometry analysis (Figures 6C–D). We show that pharmacological sEH inhibition significantly decreased the percentage of $MHCII^+$, $CD80^+$, and $CD86^+$ cells in the $CD11b^+$ gated M1-stimulated macrophages ($P<0.05$; Figure 6E). Likewise, the EETs significantly reduce the percentage of $CD80^+$, $CD86^+$, and $MHCII^+$ cells in the $CD11b^+$ gate ($P<0.05$; Figure 6E). M1 macrophages, phenotypically, express high histocompatibility complex class II (MHC-II) and CD80/86 costimulatory molecules, which are antigen-presenting components and important M1 signatures. In M2-stimulated macrophages, the percentage of $CD206^+$ in $CD11b^+$ gate did not change among the treated

groups compared to M2-stimulated alone (P>0.05; Figure 6F). However, the percentage of $MHCII^+$ and $CD80^+$ cells in the $CD11b^+$ gate in M2-stimulated macrophages was significantly increased by the EETs, while sEH inhibition only augmented the percentage of $CD80^+$ cells in the $CD11b^+$ gate (P<0.05; Figure 6E).

We then analyzed transcription factors and target genes associated with macrophage phenotype (Figure 7). **Panel A** represents the targets involved in M1-macrophages and **panel B** represents the M2-macrophages. We show that the inhibition of sEH and the EET-mix suppressed M1-macrophage phenotype by abolishing iNOS, TNF-α, IL-1β, and PTGS2/COX-2 gene expression (P<0.05; Figure 7A). Interestingly, the treatments did not affect the expression of IL-6 (P>0.05; Supplementary Figure 6A), which followed the same pattern observed *in vivo*, where the combination augmented the gingival expression of IL-6 (P<0.05; Supplementary Figure 4G). Conversely, in M2-stimulated macrophages, the inhibition of sEH and EET-mix enhances the gene expression of MRC1/CD206, Chil3/Ym1, and TGFβ1 (P<0.05; Figure 7B), whereas Arg-1 and RELMα/FIZZ1 were diminished (P<0.05; Figure 7B and Supplementary Figure 6B, respectively). Even though a few signature markers for alternatively activated macrophages are decreased or unaffected (PPAR-γ and IL-10; P>0.05; Supplementary Figure 6C – D), others are upregulated. Collectively, our data suggested that the sEH inhibition and EET-mix counteracted the classical macrophage activation profile suppressing the expression of inflammatory mediators. In alternatively activated macrophages, pharmacological sEH inhibition drove macrophage plasticity, enhancing Ym1 and CD206 expression.

Finally, we quantified the levels of two important pro-resolving mediator signatures for macrophages (Dalli & Serhan, 2012), LXA_4 and MaR1 in the supernatant of BMDMs primed with LPS (100 ng/ml) or with IL-4/−13 (10 ng/ml) (Figure 7C–D). Lipoxin A_4 was significantly increased in BMDMs with pharmacological sEH inhibition and EETs, than stimulated BMDMs and unstimulated cells (P<0.05; Figure 7C). Additionally, sEH inhibition triggered elevated levels of LXA_4 compared to EET-mix alone (P<0.05; Figure 7C).

Likewise, EETs significantly boosted the levels of MaR1 in M1- and M2-stimulated macrophages, while the sEH inhibitor solely increased in M2-stimulated macrophages (P<0.05; Figure 7D). Taken together, pharmacological sEH inhibition improved lipoxin synthesis from arachidonic acid and maresin synthesis from docosahexaenoic acid (DHA) in BMDMs macrophages, supporting the crosstalk between sEH inhibition and SPMs.

4. DISCUSSION AND CONCLUSIONS

Accumulated evidence suggests that pharmacological sEH inhibition contributes to the control of pain and chronic inflammatory disorders (Inceoglu et al., 2007; Trindade-da-Silva et al., 2020). It has been demonstrated that by inhibiting sEH, EET isomer levels as well as other EpFA, are enhanced in blood and tissue (Rose et al., 2010). To our knowledge, sEH inhibition is not uniquely involved in endogenous EET levels by the CYP450 pathway, as it was also shown to improve aspirin-triggered 15-Epi-LXA_4 production (Ono et al., 2014). However, the control of production of EpFA by modulation of cytochrome P450 is poorly

understood. Here, we reveal that pharmacological sEH inhibition has a definitive impact on other PUFA-derived metabolites, including lipoxins (LXA_4) resolvins (RvE1 and RvE2) and omega-3 fatty acid intermediates (4-HDoHE), and promotes gingival macrophage plasticity, providing a singular mechanism for preventing and resolving inflammatory osteolytic disorders. These inhibitors are currently under clinical development; therefore, uncovering their mechanism of action is crucial to define their therapeutic use.

We have previously reported that pharmacological sEH inhibition prevented alveolar bone loss in *A. actinomycetemcomitans*-induced periodontal disease (Trindade-da-Silva et al., 2017; Napimoga et al., 2018). Specifically, the pharmacological sEH inhibition and knockout animals (sEH−/−) diminish RANK/RANKL axis activation, prevented phosphorylation of endoplasmic reticulum stress sensors, and mitogen-activated protein kinase phosphorylation (p38 and JNK 1/2) (Trindade-da-Silva et al., 2017; Napimoga et al., 2018). It is essential to note that sEH expression is enhanced in inflamed gingival tissue. Consistent with the other periodontitis models (Trindade-da-Silva et al., 2017; Napimoga et al., 2018) and osteolytic models like arthritis (Trindade-da-Silva et al., 2020; Teixeira et al., 2020; Gowler et al., 2021; Tucker et al., 2021), we show that pharmacological sEH ablation prevents alveolar bone loss and dampens gingival mRNA expression of IL-17A, RANK, RANKL, and EPXH2, which are osteoclast-related activity markers. The decreased gene expression of EPXH2 should be interpreted as an indirect effect of sEH inhibition, whereby preventing EpFA degradation and inducing inflammation resolution, enhancement of sEH levels is prevented. It is also important to highlight that the combination of sEH inhibitor and EETs did not improve the prevention of bone loss or promote bone formation in our study. In fact, μCT analysis revealed that although the combination prevents bone loss, the bone volume is not maintained as well as it is with sEH inhibition alone. Additionally, elevated expression of IL-6 was found in the combination group, which is known to drive bone loss, although more recent work describes dual functionalities for IL-6 (Blanchard et al., 2009). sEH $^{-}/^{-}$ KO mice naturally presented with less bone volume than wild-type animals (Trindade-da-Silva et al., 2017).

The cytochrome P450 metabolizes PUFAs (omega-3 and −6 fatty acids) into bioactive lipids, including EETs and other EpFA (Imig & Hammock, 2009; Hashimoto, 2019). sEH was first described in mouse liver (Hammock et al., 1976) and later was pointed to as responsible for converting EETs into their inactive diol form. Since then, sEH inhibitors have emerged and brought new therapeutic perspectives in inflammation resolution (Wagner et al., 2017). In this regard, little is known about the impact of sEH inhibition on SPM production. Herein, through saliva lipidomic analyses, we show that pharmacological sEH inhibition stimulates LXA_4, RvE1, RvE2, and 4-HDoHE biosynthesis. Both RvEs counteract proinflammatory eicosanoids with concomitant resolution of inflammation actions through macrophage uptake of debris and apoptotic cells and inhibition of unwanted leukocyte traffic (Serhan & Levy, 2018). For instance, RvE1 dramatically prevents human neutrophil superoxide generation (Hasturk et al., 2006), prevents osteoclast-mediated bone resorption (Hasturk et al., 2007; El Kholy et al., 2018), inhibits effector Th17 cells, and restores the balance between effector and regulatory T cells (Alvarez et al., 2021; Oner et al., 2021). Furthermore, RvE1 in combination with LXA_4 protects against neuroinflammation in the hippocampus in a murine model of Alzheimer's disease (Kantarci et al., 2018),

and prevents migration of dendritic and γδ T cells in the epidermis of a mouse psoriasis model, controlling IL-23/IL-17 production (Sawada et al., 2018), and induces intestinal mucosa repair (Quiros et al., 2020). Previously, our group also reported that the inhibition of sEH ameliorates hyperalgesia, edema, and decreases the expression of important pro-inflammatory cytokines (Th1 and Th17), while increasing Treg cells in a mouse model of arthritis (Trindade-da-Silva et al., 2020). Similarly, 4-HDoHE, a DHA-derived metabolite, exhibited increased biosynthesis and is related to homeostatic and reparative features through peroxisome proliferator-activated receptor-gamma (PPARγ) activation (Chistyakov et al., 2020). Recently, gingival biopsies from patients with periodontitis were shown to exhibit lower expression of LTB_4 receptor 1 (BLT1/LTB4R), but not Chemerin Receptor 23 (ChemR23/CMKLR1/ERV1) (Ferguson et al., 2020), to which E-series resolvins show selective binding (Arita et al., 2007; Oh et al., 2012). Thus, pharmacological sEH inhibition improves SPM bioavailability in saliva and enhances the gingival SPM receptors, specifically RvE1, RvE2, LXA_4, and 4-HDoHE, which is consistent with the resolution of inflammation outcomes in the periodontitis model, representing a potential immune-resolvent approach that can complement conventional clinical procedures, which are often unsuccessful.

The host immune-inflammatory response drives the interplay between tissue destruction or integrity and resolution actions. In this scenario, T cells have been suggested to be the focused cell targets to prevent alveolar bone loss progression (Garlet & Giannobile, 2018). Aside from this “T-centric” framework, other types of cells display important roles in periodontal disease pathogenesis, including macrophages (Garlet & Giannobile, 2018). Macrophage phenotypic shifting is a dynamic and reversible process. For instance, resolving macrophages acquire efferocytosis functions, alter their immunometabolism pattern, produce several soluble mediators (e.g., eicosanoids, cytokines, SPMs) that dampen ongoing inflammation and support restoration of tissue integrity (Serhan & Levy, 2018; Russell, Huang & Vanderven, 2019; Ross, Devitt & Johnson, 2021). Here, our data clearly demonstrate that pharmacological sEH inhibition stimulates a dynamic process of transcriptional reprogramming of inflammatory macrophages toward resolving macrophages by enhancing $CD11c^+/CD206^+$ double-positive cells and increasing arginase 1, mannose receptor 1 (Mrc1), resistin-like α (Retnla, Fizz1), and transforming growth factor-beta (TGF-β), which is an M2 macrophage-specific gene signature. In addition to driving M2 features, pharmacological inhibition also regulates the hyperactivity of M1 macrophages, by abolishing cytokine secretion (IL-1β, TNFα, IL-12, and NOS2), and reducing the percentage of $MHCII^+$.

The *in vitro* analyses in this study also offer important insights. CD80 is one of the costimulatory molecules of the B7 family that regulates the transition between the innate and adaptive immune responses. The complex of CD80 and CD86 has two binding targets on T-cells. First, it binds to CD28 on T-cells, which activates and stimulates proliferation, differentiation, and effector functions (Lenschow, Walunas & Bluestone, 1996). Second, CD80/86 can interact with cytotoxic T-lymphocyte antigen 4 (CTLA-4) expressed on the T cell surface, inducing inhibitory signaling. The inhibitory signaling reduces IL-2 production and arrests T-cells at the G1 phase of the cell cycle (Krummel & Allison, 1995; Alegre, Frauwirth & Thompson, 2001). Also, in LPS-stimulated human macrophages, the CD80/

CD86 complex synergizes with the Toll-like receptor 4 (TLR-4) pathway regulating IL-10 and IL-27 synthesis, but not IL-12 and IL-23 (Woldai, 2014). These findings suggest that CD80/86 is influenced by sEH inhibition and the combination of sEH inhibition and EETs, and the response pattern is affected by the macrophage subtype. In the inflammatory environment (LPS-stimulated), sEH inhibition and the combination of sEH inhibition EETs downregulates the expression of CD80/86, controlling T-cell activation, and consequently the uncontrolled adaptative immune response. On the other hand, in a homeostatic and reparative environment (IL-4/−13 stimulated), the combination of sEH inhibition and ETTs upregulates the expression of CD80, which could represent, from an *in vivo* perspective, an interaction with T-cells through CTLA-4, avoiding uncontrolled T-cell activation. However, further experiments are needed to explain how CD80/86 signaling is involved with sEH inhibitors or EETs.

Pharmacological sEH inhibition enhanced Ym1 gene expression in M2-stimulated macrophages. Ym-1 has been associated with resolution functions in inflammation and tissue repair (Ikeda et al., 2018), and its silencing aggravates the severity of experimental autoimmune encephalomyelitis (EAE) (Starossom et al., 2019). Furthermore, Ym1 is considered a signature marker of alternatively activated macrophages, along with CD206 (Gordon & Martinez, 2010; Zhu et al., 2020). In agreement with the *in vivo* findings, increased levels of LXA_4 found in macrophages treated with the sEH inhibitor and the combination of sEH inhibitor and EETs are a lipid signature for M2-macrophages, as is maresin 1 (MaR1). Collectively, our data suggest that pharmacological sEH inhibition and the combination of sEH inhibitor and EETs counteracts the classical activation profile of macrophages, blocking the expression of inflammatory mediators. In alternatively activated macrophages, Ym1 and CD206 seem to be involved in improving homeostatic and reparative features, including the biosynthesis of SPMs by macrophages treated with sEH inhibitor and the combination of sEH inhibitor and EETs.

Taken together, our *in vivo* and *in vitro* findings show that pharmacological sEH inhibition prevents bone resorption in a murine periodontitis model by dampening the cytokine and eicosanoid storm, concomitant with an alteration in the lipid mediator profile, stimulating mainly E-series resolvins and LXA_4 synthesis, as well as upregulation of their receptors. We also highlight that sEH inhibition promotes macrophage plasticity, favoring resolving macrophage phenotypes.

Supplementary Material

Refer to Web version on PubMed Central for supplementary material.

Acknowledgements

This work was supported in part by USPHS grant DE025020 from NIDCR (to T.V.D.), by São Paulo Research Foundation (FAPESP) grants #2017/22334–9 and #2019/22645–0 (to M.H.N. and H.B.A., respectively), and by the National Institute of Environmental Health Sciences (NIEHS) River Award R35 ES030443–01 and NIEHS Superfund Program P42 ES004699 (to B.D.H.). We would like to thank Yoganathan Subbiah for technical support and animal care. We also thank Dr. Theodore Harris for his assistance with μCT scans.

Data Availability Statement

The data that support the findings of this study are available from the corresponding author upon reasonable request. Some data may not be made available because of privacy or ethical restrictions.

Abbreviations

TPPU-1	(1-propanoylpiperidin-4-yl)-3-[4-(trifluoromethoxy)phenyl]urea
4-HDoHE	4-hydroxy docosahexaenoic acid
AA	Arachidonic acid
Arg-1	Arginase-1
CEJ	Cementoenamel junction
CMKLR1/ChemR23	Chemokine like receptor 1 or Chemerin Receptor 23
Chil3/Ym1	Chitinase-like 3
CTLA-4	cytotoxic T-lymphocyte antigen 4
DHETs	Dihydroxyeicosatrienoic acids
DHA	Docosahexaenoic acid
EPA	Eicosapentaenoic acid
ER	Endoplasmic reticulum
EPXH2	epoxide hydrolase 2
EpFA	Epoxy fatty acids
EETs	Epoxyeicosatrienoic acids
iNOS	Inducible nitric oxide synthases
LTB4R1	Leukotriene B4 receptor 1
LMs	Lipid mediators
LX	Lipoxins
MHCII	Major histocompatibility complex II
MaR1	Maresin 1
mEH	Microsomal epoxide hydrolase
FPR2	N-formyl peptide receptor 2

OPG	osteoprotegerin
PPARγ	Peroxisome Proliferator-Activated Receptor Gamma
PUFA	Polyunsaturated fatty acid
RANKL	receptor activator of nuclear factor-kappa beta ligand
Retnla/ FIZZ1	Resistin-like molecule alpha
RvD	Resolvin D-series
RvE	Resolvin E-series
SPMs	Specialized pro-resolving mediators

REFERENCES

1. Alegre ML, Frauwirth KA, Thompson CB. T-cell regulation by CD28 and CTLA-4. Nat Rev Immunol. 2001 Dec;1(3):220–8. [PubMed: 11905831]
2. Alexander SP, Christopoulos A, Davenport AP, Kelly E, Mathie A, Peters JA, Veale EL et al. (2021) THE CONCISE GUIDE TO PHARMACOLOGY 2021/22: G protein-coupled receptors. Br J Pharmacol. 176 Suppl 1:S27–S156.
3. Alexander SP, Doherty P, Fairlie D, Fowler CJ, Overall CM, Rawlings N, Southan C, Turner AJ. Hydrolases (version 2019.5) in the IUPHAR/BPS Guide to Pharmacology Database. IUPHAR/BPS Guide to Pharmacology CITE. 2019; 2019(5).
4. Alexander SP, Fabbro D, Kelly E, Mathie A, Peters JA, Veale EL et al. (2021) THE CONCISE GUIDE TO PHARMACOLOGY 2021/22: Enzymes. Br J Pharmacol. 178 Suppl 1:S313–S411. [PubMed: 34529828]
5. Alvarez C, Abdalla H, Sulliman S, Rojas P, Wu YC, Almarhoumi R, Huang RY, Galindo M, Vernal R, Kantarci A. RvE1 Impacts the Gingival Inflammatory Infiltrate by Inhibiting the T Cell Response in Experimental Periodontitis. Front Immunol. 2021 May 3; 12:664756. [PubMed: 34012448]
6. Alvarez C, Monasterio G, Cavalla F, Córdova LA, Hernández M, Heymann D, Garlet GP, Sorsa T, Pärnänen P, Lee HM, Golub LM, Vernal R, Kantarci A. Osteoimmunology of Oral and Maxillofacial Diseases: Translational Applications Based on Biological Mechanisms. Front Immunol. 2019 Jul 18; 10:1664. [PubMed: 31379856]
7. Arita M, Ohira T, Sun YP, Elangovan S, Chiang N, Serhan CN. Resolvin E1 selectively interacts with leukotriene B4 receptor BLT1 and ChemR23 to regulate inflammation. J Immunol. 2007 Mar 15;178(6):3912–7. [PubMed: 17339491]
8. Bäck M, Brink C, Chiang N, Dahlén SE, Dent G, Drazen J, Evans JF, Hay DWP, Nakamura M, Powell W, Rokach J, Rovati GE, Serhan CN, Shimizu T, Uddin M, Yokomizo T. Leukotriene receptors (version 2020.3) in the IUPHAR/BPS Guide to Pharmacology Database. IUPHAR/BPS Guide to Pharmacology CITE. 2020; 2020(3).
9. Balta MG, Papathanasiou E, Blix IJ, Van Dyke TE. Host Modulation and Treatment of Periodontal Disease. J Dent Res. 2021 Jul;100(8):798–809. [PubMed: 33655803]
10. Blanchard F, Duplomb L, Baud'huin M, Brounais B. The dual role of IL-6-type cytokines on bone remodeling and bone tumors. Cytokine Growth Factor Rev. 2009 Feb;20(1):19–28. [PubMed: 19038573]
11. Chistyakov DV, Astakhova AA, Goriainov SV, Sergeeva MG. Comparison of PPAR Ligands as Modulators of Resolution of Inflammation, via Their Influence on Cytokines and Oxylipins Release in Astrocytes. Int J Mol Sci. 2020 Dec 16;21(24):9577. [PubMed: 33339154]
12. Dalli J, Serhan C. Macrophage Proresolving Mediators-the When and Where. Microbiol Spectr. 2016 Jun;4(3): 10.1128/microbiolspec.MCHD-0001-2014.

13. Dalli J, Serhan CN. Specific lipid mediator signatures of human phagocytes: microparticles stimulate macrophage efferocytosis and pro-resolving mediators. Blood. 2012 Oct 11;120(15): e60–72. [PubMed: 22904297]

14. El Kholy K, Freire M, Chen T, Van Dyke TE. Resolvin E1 Promotes Bone Preservation Under Inflammatory Conditions. Front Immunol. 2018 Jun 12; 9:1300. [PubMed: 29946319]

15. Ferguson B, Bokka NR, Maddipati KR, Ayilavarapu S, Weltman R, Zhu L, Chen W, Zheng WJ, Angelov N, Van Dyke TE, Lee CT. Distinct Profiles of Specialized Pro-resolving Lipid Mediators and Corresponding Receptor Gene Expression in Periodontal Inflammation. Front Immunol. 2020 Jun 25; 11:1307. [PubMed: 32670289]

16. Fishbein A, Hammock BD, Serhan CN, Panigrahy D. Carcinogenesis: Failure of resolution of inflammation? Pharmacol Ther. 2021 Feb; 218:107670. [PubMed: 32891711]

17. Fishbein A, Wang W, Yang H, Yang J, Hallisey VM, Deng J, Verheul SML, Hwang SH, Gartung A, Wang Y, Bielenberg DR, Huang S, Kieran MW, Hammock BD, Panigrahy D. Resolution of eicosanoid/cytokine storm prevents carcinogen and inflammation-initiated hepatocellular cancer progression. Proc Natl Acad Sci U S A. 2020 Sep 1;117(35):21576–21587. doi: 10.1073/pnas.2007412117. [PubMed: 32801214]

18. Garlet GP, Giannobile WV. Macrophages: The Bridge between Inflammation Resolution and Tissue Repair? J Dent Res. 2018 Sep;97(10):1079–1081. [PubMed: 29993304]

19. Gartung A, Yang J, Sukhatme VP, Bielenberg DR, Fernandes D, Chang J, Schmidt BA, Hwang SH, Zurakowski D, Huang S, Kieran MW, Hammock BD, Panigrahy D. Suppression of chemotherapy-induced cytokine/lipid mediator surge and ovarian cancer by a dual COX-2/sEH inhibitor. Proc Natl Acad Sci U S A. 2019 Jan 29;116(5):1698–1703. doi: 10.1073/pnas.1803999116. [PubMed: 30647111]

20. Gerlier D, and Thomasset N. Use of MTT colorimetric assay to measure cell activation. J Immunol Methods. (1986) 94:57–63. Doi: 10.1016/0022-1759(86)90215-2. [PubMed: 3782817]

21. Gordon S, Martinez FO. Alternative activation of macrophages: mechanism and functions. Immunity. 2010 May 28;32(5):593–604. [PubMed: 20510870]

22. Gowler PRW, Turnbull J, Shahtaheri M, Gohir S, Kelly T, McReynolds C, Jun Y, Jha RR, Fernandes GS, Zhang W, Doherty M, Walsh DA, Bruce HD, Valdes AM, Barrett DA, Chapman V. Clinical and preclinical evidence for roles of soluble epoxide hydrolase in osteoarthritis knee pain. Arthritis Rheumatol. 2021 Oct 21.

23. Hajishengallis G, Chavakis T. Local and systemic mechanisms linking periodontal disease and inflammatory comorbidities. Nat Rev Immunol. 2021 Jul;21(7):426–440. [PubMed: 33510490]

24. Hammock BD, Gill SS, Stamoudis V, Gilbert LI. Soluble mammalian epoxide hydratase: action on juvenile hormone and other terpenoid epoxides. Comp Biochem Physiol B. 1976;53(2):263–5. [PubMed: 1253563]

25. Hammock BD, Wang W, Gilligan MM, Panigrahy D. Eicosanoids: The Overlooked Storm in Coronavirus Disease 2019 (COVID-19)? Am J Pathol. 2020 Sep;190(9):1782–1788. [PubMed: 32650004]

26. Hashimoto K Role of Soluble Epoxide Hydrolase in Metabolism of PUFAs in Psychiatric and Neurological Disorders. Front Pharmacol. 2019 Jan 30; 10:36. [PubMed: 30761004]

27. Hasturk H, Kantarci A, Goguet-Surmenian E, Blackwood A, Andry C, Serhan CN, Van Dyke TE. Resolvin E1 regulates inflammation at the cellular and tissue level and restores tissue homeostasis in vivo. J Immunol. 2007 Nov 15;179(10):7021–9. [PubMed: 17982093]

28. Hasturk H, Kantarci A, Ohira T, Arita M, Ebrahimi N, Chiang N, Petasis NA, Levy BD, Serhan CN, Van Dyke TE. RvE1 protects from local inflammation and osteoclast- mediated bone destruction in periodontitis. FASEB J. 2006 Feb;20(2):401–3. [PubMed: 16373400]

29. Hildreth K, Kodani SD, Hammock BD, Zhao L. Cytochrome P450-derived linoleic acid metabolites EpOMEs and DiHOMEs: a review of recent studies. J Nutr Biochem. 2020 Dec; 86:108484. [PubMed: 32827665]

30. Ikeda N, Asano K, Kikuchi K, Uchida Y, Ikegami H, Takagi R, Yotsumoto S, Shibuya T, Makino-Okamura C, Fukuyama H, Watanabe T, Ohmuraya M, Araki K, Nishitai G, Tanaka M. Emergence of immunoregulatory Ym1+Ly6Chi monocytes during recovery phase of tissue injury. Sci Immunol. 2018 Oct 5;3(28): eaat0207. [PubMed: 30291130]

31. Imig JD, and Hammock BD (2009). Soluble epoxide hydrolase as a therapeutic target for cardiovascular diseases. Nat. Rev. Drug Discov. 8, 794–805. [PubMed: 19794443]
32. Inceoglu B, Schmelzer KR, Morisseau C, Jinks SL, Hammock BD. Soluble epoxide hydrolase inhibition reveals novel biological functions of epoxyeicosatrienoic acids (EETs). Prostaglandins Other Lipid Mediat. 2007 Jan;82(1–4):42–9. [PubMed: 17164131]
33. Kantarci A, Aytan N, Palaska I, Stephens D, Crabtree L, Benincasa C, Jenkins BG, Carreras I, Dedeoglu A. Combined administration of resolvin E1 and lipoxin A4 resolves inflammation in a murine model of Alzheimer's disease. Exp Neurol. 2018 Feb; 300:111–120. [PubMed: 29126887]
34. Kilkenny C, Browne W, Cuthill IC, Emerson M, Altman DG, & Group NCRRGW (2010). Animal research: Reporting in vivo experiments: The ARRIVE guidelines. British Journal of Pharmacology, 160(7), 1577–1579. [PubMed: 20649561]
35. Krummel MF and Allison JP 1995. CD28 and CTLA-4 have opposing effects on the response of T cells to stimulation. J. Exp. Med. 182: 459–465. [PubMed: 7543139]
36. Lamont RJ & Hajishengallis G Polymicrobial synergy and dysbiosis in inflammatory disease. Trends Mol. Med. 21, 172–183 (2015). [PubMed: 25498392]
37. Lenschow DJ, Walunas TL, and Bluestone JA 1996. CD28/B7 system of T cell costimulation. Annu. Rev. Immunol. 14: 233–258. [PubMed: 8717514]
38. Marchesan J, Girnary MS, Jing L, Miao MZ, Zhang S, Sun L, Morelli T, Schoenfisch MH, Inohara N, Offenbacher S, Jiao Y. An experimental murine model to study periodontitis. Nat Protoc. 2018 Oct;13(10):2247–2267. [PubMed: 30218100]
39. McReynolds C, Morisseau C, Wagner K, Hammock B. Epoxy Fatty Acids Are Promising Targets for Treatment of Pain, Cardiovascular Disease and Other Indications Characterized by Mitochondrial Dysfunction, Endoplasmic Stress and Inflammation. Adv Exp Med Biol. 2020; 1274:71–99. [PubMed: 32894508]
40. Morisseau C, Inceoglu B, Schmelzer K, Tsai HJ, Jinks SL, Hegedus CM, Hammock BD. Naturally occurring monoepoxides of eicosapentaenoic acid and docosahexaenoic acid are bioactive antihyperalgesic lipids. J Lipid Res. 2010 Dec;51(12):3481–90. [PubMed: 20664072]
41. Napimoga MH, Rocha EP, Trindade-da-Silva CA, Demasi APD, Martinez EF, Macedo CG, Abdalla HB, Bettaieb A, Haj FG, Clemente-Napimoga JT, Inceoglu B, Hammock BD. Soluble epoxide hydrolase inhibitor promotes immunomodulation to inhibit bone resorption. J Periodontal Res. 2018 Oct; 53(5):743–749. [PubMed: 29851077]
42. Oh SF, Dona M, Fredman G, Krishnamoorthy S, Irimia D, Serhan CN. Resolvin E2 formation and impact in inflammation resolution. J Immunol. 2012 May 1;188(9):4527–34. [PubMed: 22450811]
43. Oner F, Alvarez C, Yaghmoor W, Stephens D, Hasturk H, Firatli E, Kantarci A. Resolvin E1 Regulates Th17 Function and T Cell Activation. Front Immunol. 2021 Mar 17; 12:637983. [PubMed: 33815391]
44. Ono E, Dutile S, Kazani S, Wechsler ME, Yang J, Hammock BD, Douda DN, Tabet Y, Khaddaj-Mallat R, Sirois M, Sirois C, Rizcallah E, Rousseau E, Martin R, Sutherland ER, Castro M, Jarjour NN, Israel E, Levy BD; National Heart, Lung, and Blood Institute's Asthma Clinical Research Network. Lipoxin generation is related to soluble epoxide hydrolase activity in severe asthma. Am J Respir Crit Care Med. 2014 Oct 15;190(8):886–97. [PubMed: 25162465]
45. Panigrahy D, Gilligan MM, Huang S, Gartung A, Cortés-Puch I, Sime PJ, Phipps RP, Serhan CN, Hammock BD. Inflammation resolution: a dual-pronged approach to averting cytokine storms in COVID-19? Cancer Metastasis Rev. 2020 Jun;39(2):337–340. [PubMed: 32385712]
46. Panigrahy D, Gilligan MM, Serhan CN, Kashfi K. Resolution of inflammation: An organizing principle in biology and medicine. Pharmacol Ther. 2021 Nov; 227:107879. [PubMed: 33915177]
47. Quiros M, Feier D, Birkl D, Agarwal R, Zhou DW, García AJ, Parkos CA, Nusrat A. Resolvin E1 is a pro-repair molecule that promotes intestinal epithelial wound healing. Proc Natl Acad Sci U S A. 2020 Apr 28;117(17):9477–9482. [PubMed: 32300016]
48. Rose TE, Morisseau C, Liu JY, Inceoglu B, Jones PD, Sanborn JR, Hammock BD. 1-Aryl-3-(1-acylpiperidin-4-yl)urea inhibitors of human and murine soluble epoxide hydrolase: structure-activity relationships, pharmacokinetics, and reduction of inflammatory pain. J Med Chem. 2010 Oct 14;53(19):7067–75. [PubMed: 20812725]

49. Ross EA, Devitt A, Johnson JR. Macrophages: The Good, the Bad, and the Gluttony. Front Immunol. 2021 Aug 12; 12:708186. [PubMed: 34456917]
50. Russell DG, Huang L, VanderVen BC. Immunometabolism at the interface between macrophages and pathogens. Nat Rev Immunol. 2019 May;19(5):291–304. [PubMed: 30679807]
51. Sawada Y, Honda T, Nakamizo S, Otsuka A, Ogawa N, Kobayashi Y, Nakamura M, Kabashima K. Resolvin E1 attenuates murine psoriatic dermatitis. Sci Rep. 2018 Aug 8;8(1):11873. [PubMed: 30089836]
52. Schmelzer KR, Kubala L, Newman JW, Kim IH, Eiserich JP, Hammock BD. Soluble epoxide hydrolase is a therapeutic target for acute inflammation. Proceedings of the National Academy of Sciences of the United States of America. 2005;102(28):9772–9777. [PubMed: 15994227]
53. Serhan CN, Levy BD. Resolvins in inflammation: emergence of the pro-resolving superfamily of mediators. J Clin Invest. 2018 Jul 2; 128(7):2657–2669. [PubMed: 29757195]
54. Serhan CN, Savill J. Resolution of inflammation: the beginning programs the end. Nat Immunol. 2005 Dec;6(12):1191–7. [PubMed: 16369558]
55. Serhan CN. Pro-resolving lipid mediators are leads for resolution physiology. Nature. 2014 Jun 5;510(7503):92–101. [PubMed: 24899309]
56. Starossom SC, Campo Garcia J, Woelfle T, Romero-Suarez S, Olah M, Watanabe F, Cao L, Yeste A, Tukker JJ, Quintana FJ, Imitola J, Witzel F, Schmitz D, Morkel M, Paul F, Infante-Duarte C, Khoury SJ. Chi3l3 induces oligodendrogenesis in an experimental model of autoimmune neuroinflammation. Nat Commun. 2019 Jan 15;10(1):217. [PubMed: 30644388]
57. Teixeira JM, Abdalla HB, Basting RT, Hammock BD, Napimoga MH, Clemente-Napimoga JT. Peripheral soluble epoxide hydrolase inhibition reduces hypernociception and inflammation in albumin-induced arthritis in temporomandibular joint of rats. Int Immunopharmacol. 2020 Oct; 87:106841. [PubMed: 32736189]
58. Trindade-da-Silva CA, Bettaieb A, Napimoga MH, Lee KSS, Inceoglu B, Ueira-Vieira C, Bruun D, Goswami SK, Haj FG, Hammock BD. Soluble Epoxide Hydrolase Pharmacological Inhibition Decreases Alveolar Bone Loss by Modulating Host Inflammatory Response, RANK-Related Signaling, Endoplasmic Reticulum Stress, and Apoptosis. J Pharmacol Exp Ther. 2017 Jun; 361(3):408–416. [PubMed: 28356494]
59. Trindade-da-Silva CA, Clemente-Napimoga JT, Abdalla HB, Rosa SM, Ueira-Vieira C, Morisseau C, Verri WA Jr, Montalli VAM, Hammock BD, Napimoga MH. Soluble epoxide hydrolase inhibitor, TPPU, increases regulatory T cells pathway in an arthritis model. FASEB J. 2020 Jul;34(7):9074–9086. [PubMed: 32400048]
60. Tucker L, Trumble TN, Groschen D, Dobbs E, Baldo CF, Wendt-Hornickle E, Guedes AGP. Targeting Soluble Epoxide Hydrolase and Cyclooxygenases Enhance Joint Pain Control, Stimulate Collagen Synthesis, and Protect Chondrocytes From Cytokine-Induced Apoptosis. Front Vet Sci. 2021 Aug 5; 8:685824. [PubMed: 34422942]
61. Van Dyke TE, Bartold PM, Reynolds EC. The Nexus Between Periodontal Inflammation and Dysbiosis. Front Immunol. 2020 Mar 31; 11:511. [PubMed: 32296429]
62. Van Dyke TE, Sima C. Understanding resolution of inflammation in periodontal diseases: Is chronic inflammatory periodontitis a failure to resolve? Periodontol 2000. 2020 Feb;82(1):205–213. [PubMed: 31850636]
63. Van Dyke TE. Shifting the paradigm from inhibitors of inflammation to resolvers of inflammation in periodontitis. J Periodontol. 2020 Oct;91 Suppl 1(Suppl 1): S19–S25. [PubMed: 32441774]
64. Viniegra A, Goldberg H, Çil Ç, Fine N, Sheikh Z, Galli M, Freire M, Wang Y, Van Dyke TE, Glogauer M, Sima C. Resolving Macrophages Counter Osteolysis by Anabolic Actions on Bone Cells. J Dent Res. 2018 Sep;97(10):1160–1169. [PubMed: 29993312]
65. Wagner KM, McReynolds CB, Schmidt WK, Hammock BD. Soluble epoxide hydrolase as a therapeutic target for pain, inflammatory and neurodegenerative diseases. Pharmacol Ther. 2017 Dec; 180:62–76. [PubMed: 28642117]
66. Wang D, Dubois RN. Eicosanoids and cancer. Nat Rev Cancer. 2010 Mar;10(3):181–93. [PubMed: 20168319]
67. Woldai S (2014). The Role of CD80 and CD86 In Macrophage Activation and its Regulation Following LPS Stimulation.

68. Xia J, Wishart D Web-based inference of biological patterns, functions and pathways from metabolomic data using MetaboAnalyst. Nat Protoc 6, 743–760 (2011). [PubMed: 21637195]

69. Ying W, Cheruku PS, Bazer FW, Safe SH, Zhou B. Investigation of macrophage polarization using bone marrow derived macrophages. J Vis Exp. 2013 Jun 23;(76):50323. [PubMed: 23851980]

70. Zeldin DC. Epoxygenase pathways of arachidonic acid metabolism. J Biol Chem. 2001 Sep 28;276(39):36059–62. [PubMed: 11451964]

71. Zhu W, Lönnblom E, Förster M, Johannesson M, Tao P, Meng L, Lu S, Holmdahl R. Natural polymorphism of Ym1 regulates pneumonitis through alternative activation of macrophages. Sci Adv. 2020 Oct 21;6(43): eaba9337. [PubMed: 33087360]

What is already known

Inhibition of soluble epoxide hydrolase prevents bone resorption.

What this study adds

sEH inhibition drives specialized pro-resolving lipid mediators production, concomitant with up-regulation of SPM receptors.

Resolving macrophages plasticity is stimulated by sEH inhibition.

Clinical significance

sEH inhibition stimulates resolution of inflammation pathways as an immunoresolvent, not as an immunosuppressive agent.

Pharmacological sEH inhibition might be useful for management of osteolytic inflammatory diseases.

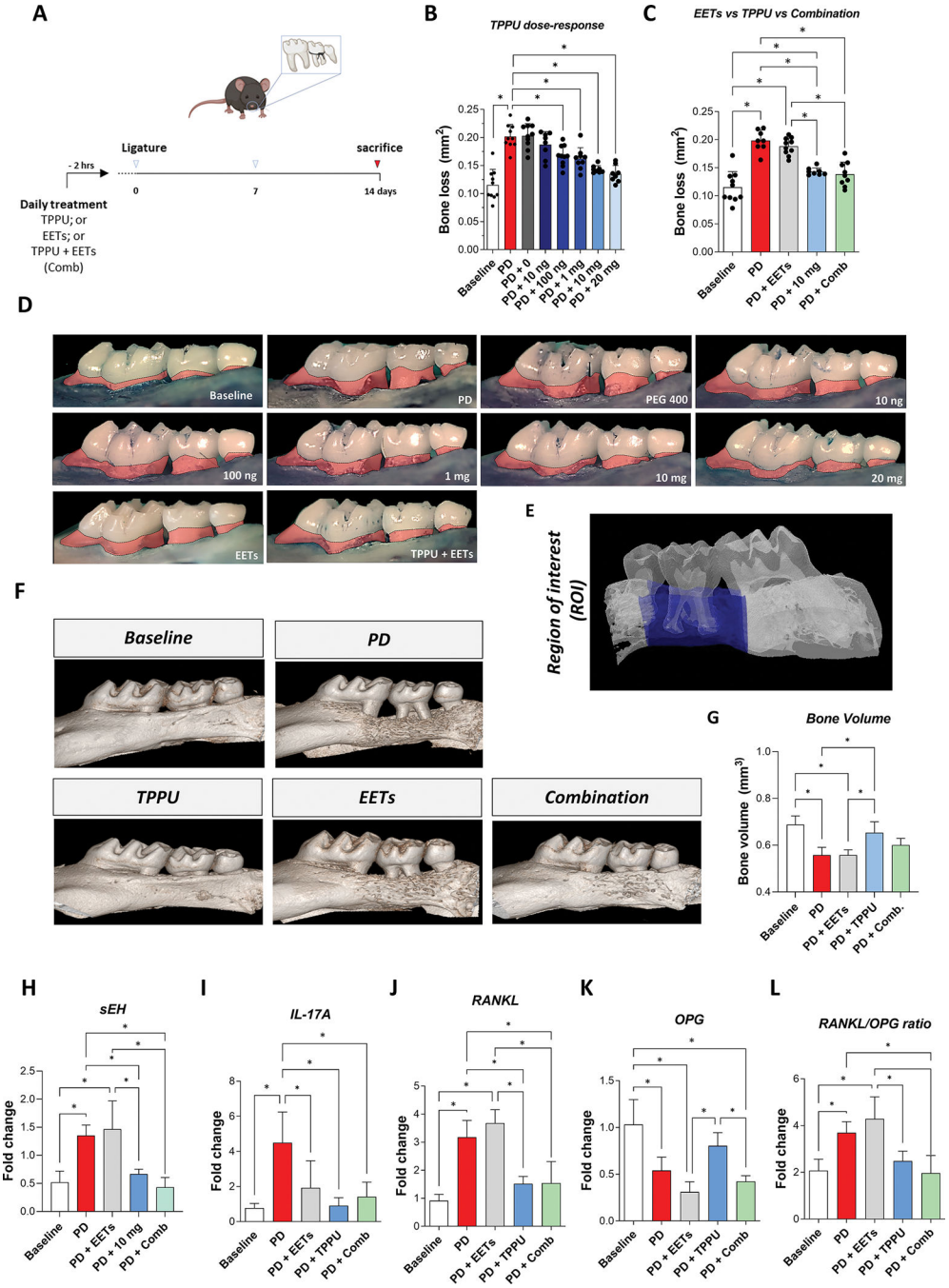

Figure 1. Inhibition of soluble epoxide hydrolase prevents experimental periodontitis bone loss and reduces hallmark osteolytic cytokines.

(A) Experimental design flowchart. **(B)** Bone loss was quantified as the area (mm^2) between the cementum-enamel junction and the alveolar bone in animals treated with or without sEH inhibitor (TPPU); **(C)** or in animals treated with epoxyeicosatrienoic acids (EETs) and EETs plus sEH inhibitor (Combination). **(D)** Representative images from a palatal view of maxillary molars. The areas measured are highlighted in light red. Micro–computed tomography (microCT) was used to quantify bone volume. **(E)** The region of

interest is identified in blue and **(F)** bone volume was measured. **(G)** Representative microCT-3-dimensional reconstruction images of vestibular maxillary molars. Gingival mRNA expression of **(H)** soluble epoxy hydrolase (sEH), **(I)** IL-17A, **(J)** RANKL, **(K)** OPG, and **(L)** RANKL/OPG ratio. *P < 0.05, **P < 0.01, ***P < 0.001, ****P < 0.0001. The data are expressed as mean ± S.D.; n = 5 animals per group.

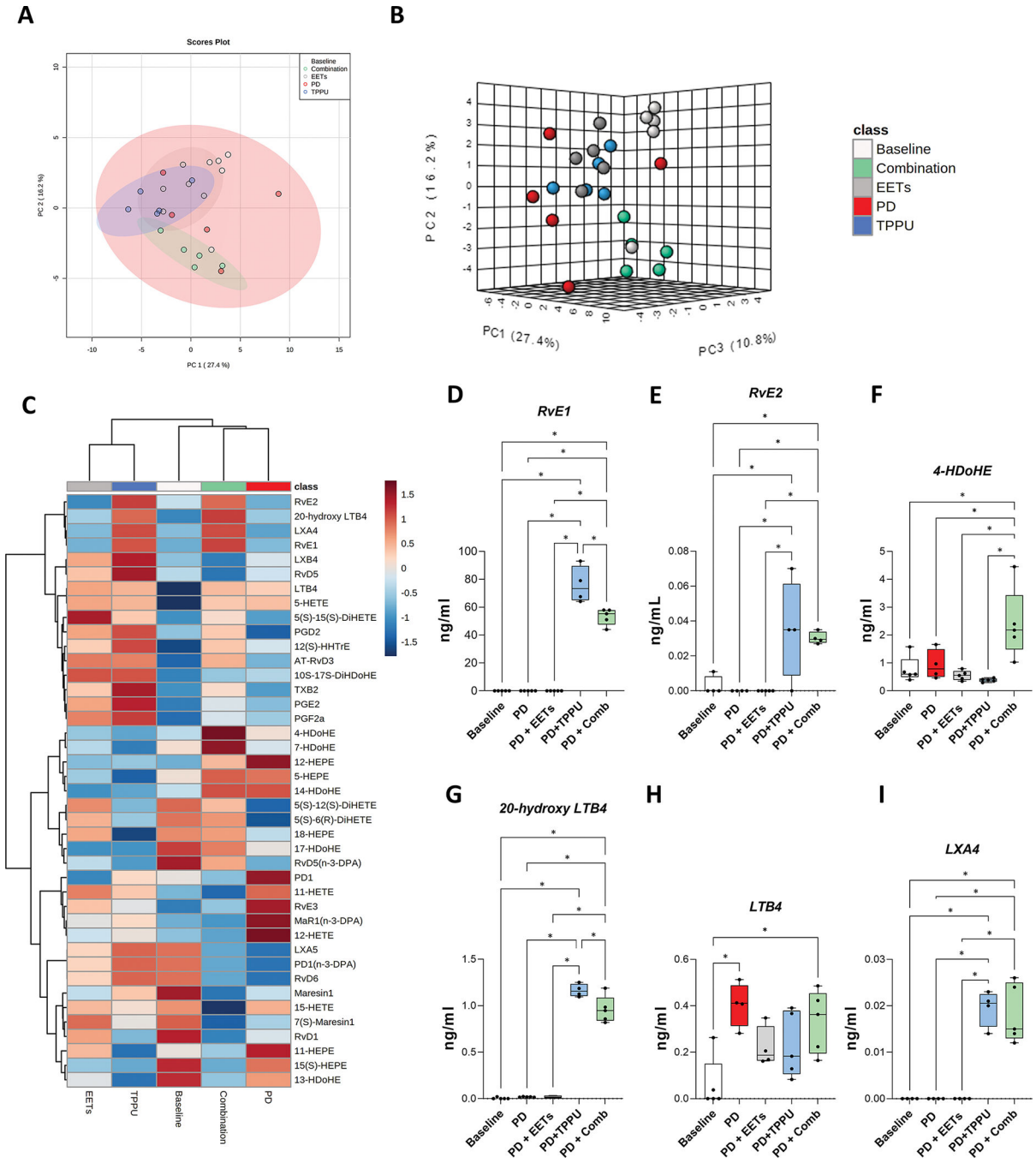

Figure 2. sEH enzyme suppression promotes Resolvin E-series and Lipoxin A4 production in saliva.

Principal component analysis (PCA) graph in **(A)** two-dimensions and **(B)** three-dimensions for the profiles of specialized pro-resolution lipid mediators (SPMs) and lipid mediators (LMs) in the saliva samples of mice. Each point represents a sample in each group. This graph demonstrates groups of samples arranged according to their similarity with lipid mediator levels. White circles represent the baseline group; red circles the experimental periodontitis group; gray circles the EETs group; the blue circles the sEH inhibitor group

(TPPU); green circles the combination group. **(C)** Heatmap and clustering of specialized pro-resolution lipid mediators (SPMs) and lipid mediators (LMs). Individual box plots of **(D)** RvE1, **(E)** RvE2, **(F)** 4-HDoHE, **(G)** 20-hydroxy LTB4, **(H)** LTB4, **(I)** LXA4. *P<0.05, **P<0.01, ***P<0.001, ****P<0.0001. Data are expressed as mean ± S.D.; n = 5 animals per group.

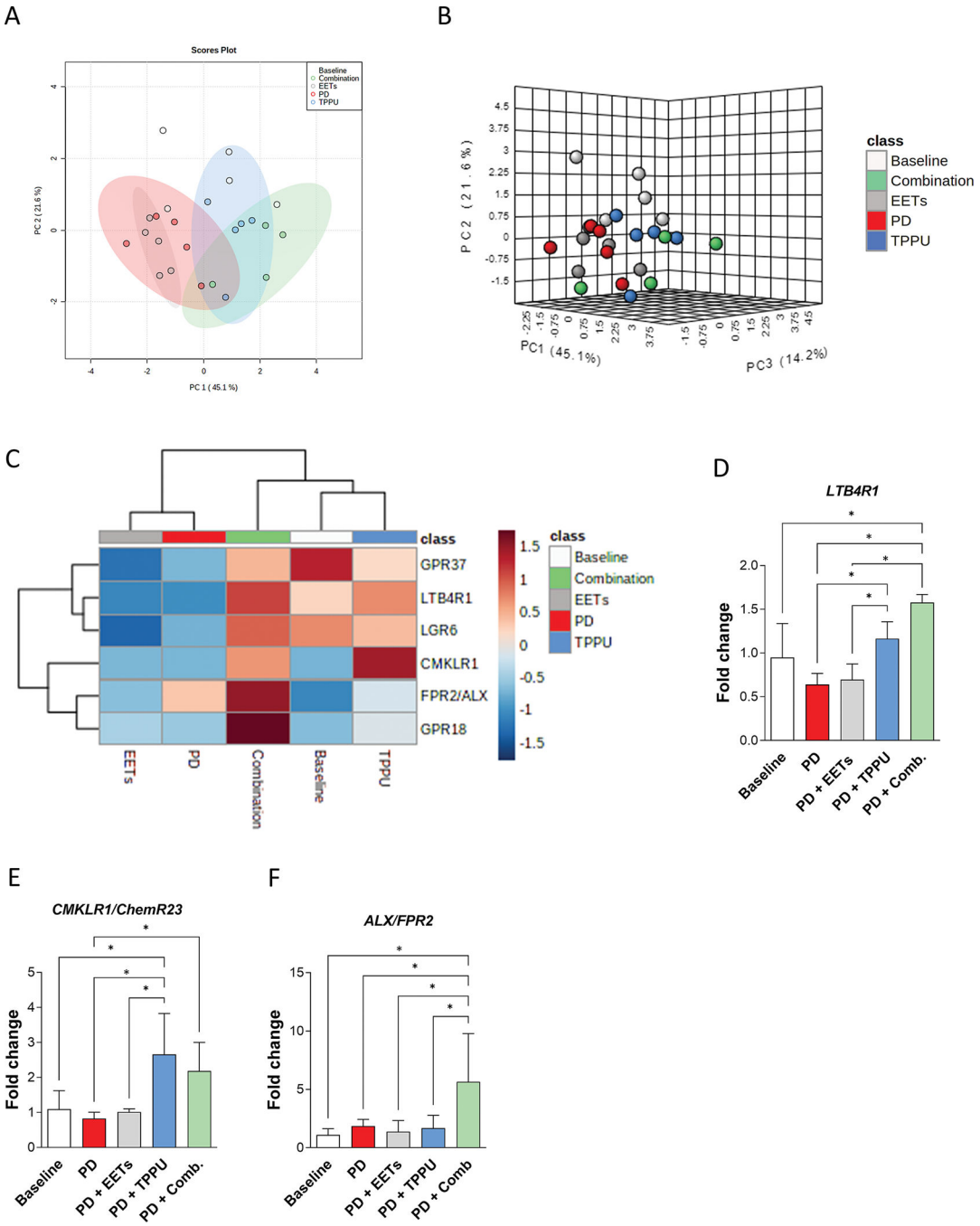

Figure 3. SPM receptors are overexpressed with sEH inhibition in gingival tissue.

Principal component analysis (PCA) graph in **(A)** two-dimensions and **(B)** three-dimensions for the specialized pro-resolution lipid mediator receptors (SPMs) in mouse gingival tissue. Each point represents a sample in each group. This graph demonstrates groups of samples based on their similarity in lipid receptor levels. White circles represent the baseline group; red circles the experimental periodontitis group; gray circles the EETs group; blue circles the sEH inhibitor group (TPPU); green circles the combination group. **(C)** Heatmap and clustering of gene expression of specialized pro-resolution lipid mediator (SPM) receptors.

Gingival mRNA expression of **(D)** LTB4R1, **(E)** CMKLR1/ChemR23, and **(F)** ALX/FPR2. *P<0.05, **P<0.01, ***P<0.001, ****P<0.0001. Data are expressed as mean ± S.D.; n = 5 animals per group.

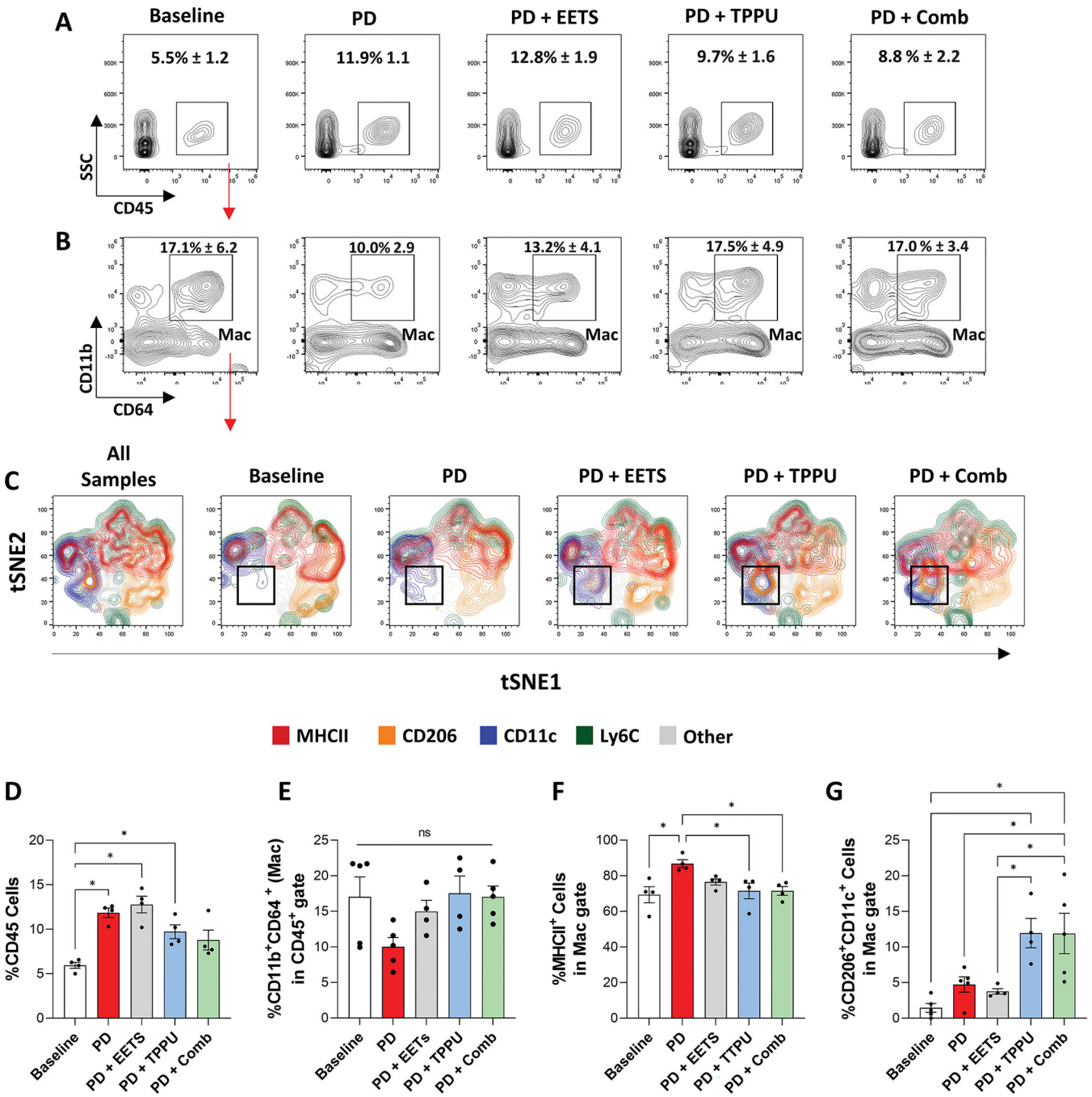

Figure 4. Impact of sEH inhibition and EETs on gingival macrophages during experimental periodontal disease.

(A) Representative contour plots indicating gingival CD45+ cells, mean frequencies (among total live gingival cells) ± SD. **(B)** Representative contour plots indicating mean frequencies among total live gingival cells ± SD of CD45+CD11b+CD64+ cells (Macrophages (Mac) gate). The red arrow indicates the gating strategy. **(C)** tSNE graphs of MAC cells (concatenated data, 4 animals per group) expressing MHCII, CD206, Ly6C and CD11c. Black square indicates CD11c+CD206+ cells. **(D-G)** Percentage frequencies of total CD45+

cells, Mac cells among CD45+, MHCII+ among Mac cells, and CD11c+CD206+ cells among Mac cells. *P < 0.05, **P < 0.01, ***P < 0.001, ****P < 0.0001. The data are expressed as mean ± S.D.

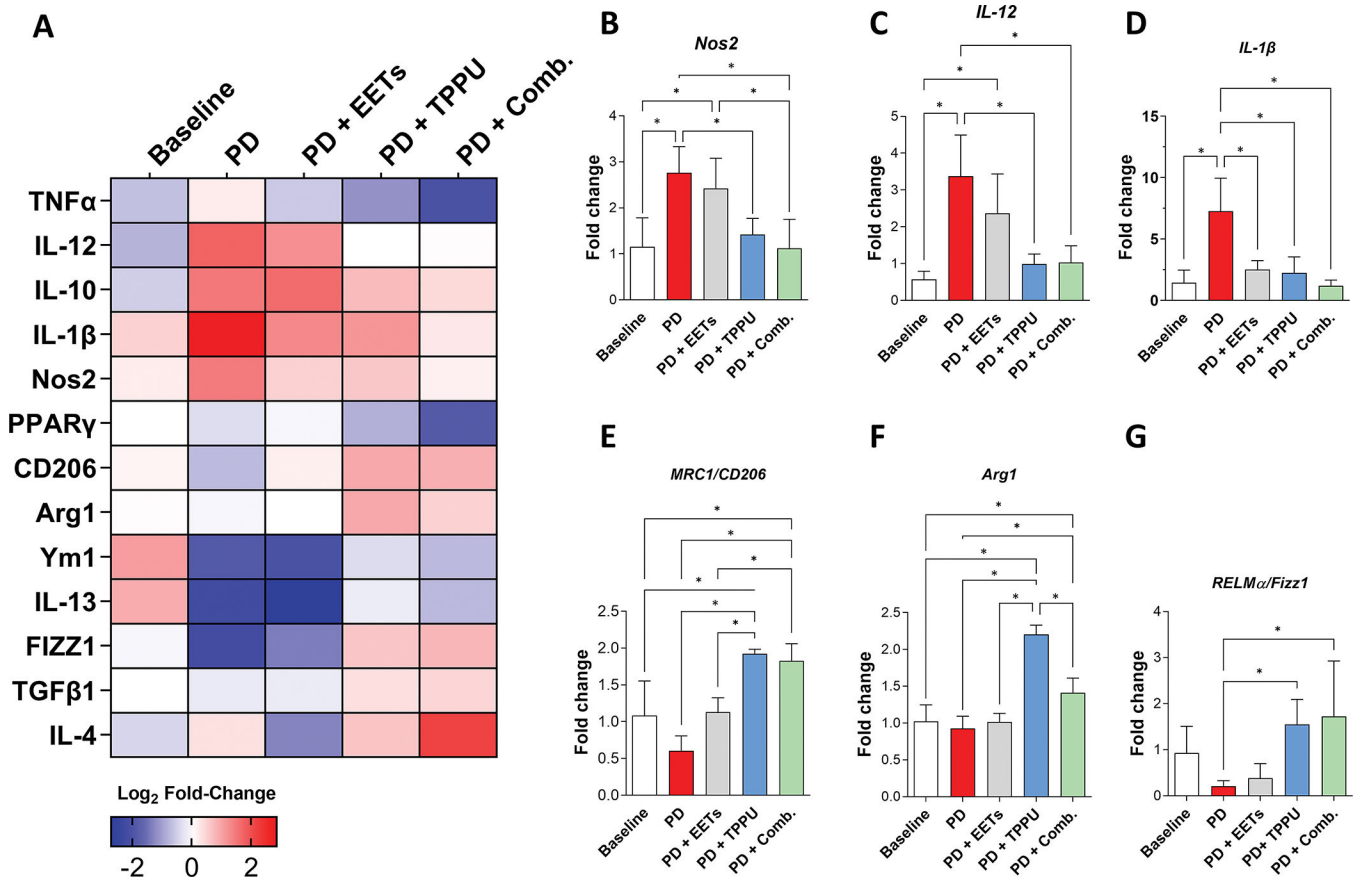

Figure 5. Suppression of signatures markers of inflammatory macrophages whereas stimulation of resolving macrophages through sEH inhibition.

(A) Heatmap representing the log2 fold-change gingival expression of mRNA of cytokines. Gingival mRNA expression of **(B)** iNOS, **(C)** IL-12, **(D)** IL-1β, **(E)** MRC1/CD206, **(F)** Arg1, and **(G)** RELMα/FIZZ1. *P < 0.05, **P < 0.01, ***P < 0.001, ****P < 0.0001. The data are expressed as mean ± S.D.; n = 5 animals per group.

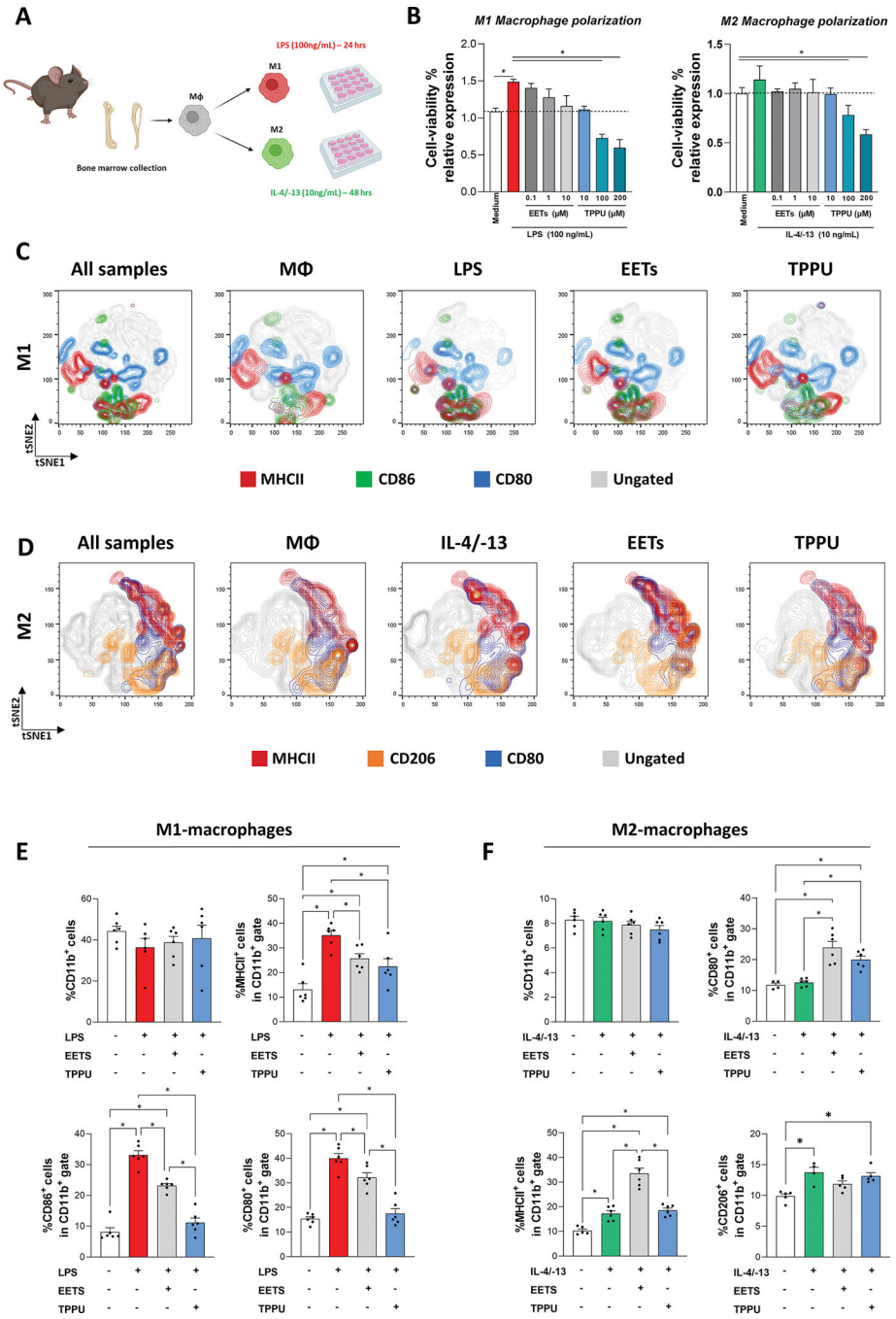

Figure 6. Inhibition of sEH impairs M1-macrophage cell-presenting features, while improving CD80/86 complexes in M2-macrophages.

(A) Experimental design: Isolated bone-marrow cells were cultured in growth medium for 7 days, followed by M1 (LPS 100ng/mL, 24 hours) or M2 (IL-4/13 10ng/mL, 48hrs) stimulation. **(B)** Cell viability was assessed by MTT assay and is presented as relative expression. **(C)** tSNE graphs of M1-stimulated or non-stimulated cells for 24 hrs (concatenated data, 5 wells per group, density at 2,5×106/well) expressing MHCII, CD11b, CD80, and CD86. **(D)** tSNE graphs of M2-stimulated or non-stimulated cells for 48hrs

(concatenated data, 5 wells per group, and density at 2,5×106/well) expressing CD11b, CD206, CD80, and CD86. **(E)** Percentages of total CD11b+ cells, MHCII+ among CD11b+ cells, CD86+ among CD11b+ cells, and CD80+ among CD11b+ cells. **(F)** Percentages of total CD11b+ cells, CD80+ among CD11b+ cells, MHCII+ among CD11b+ cells, and CD206+ among CD11b+ cells. *P < 0.05, **P < 0.01, ***P < 0.001, ****P < 0.0001. The data are expressed as mean ± S.D. n = 6 animals per group with 2 biological replicates.

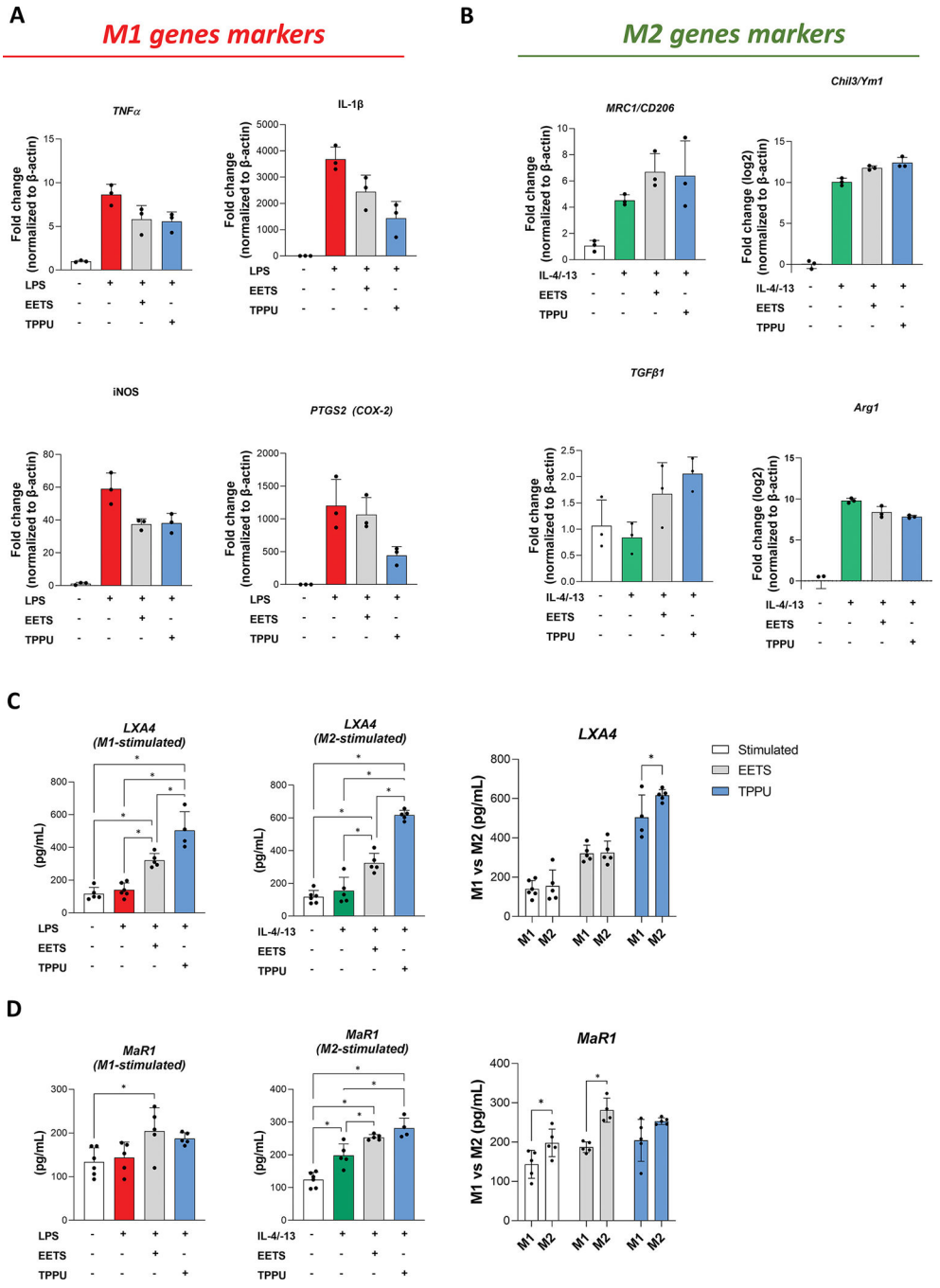

Figure 7. Impact of sEH inhibitor and EETs on gene expression of polarized macrophages, and LXA4 and MaR1 synthesis in BMDMs.

Isolated bone-marrow cells were cultured in a growth medium for 7 days followed by M1 (LPS 100ng/mL, 24 hours) or M2 (IL-4/13 10ng/mL, 48hrs) stimulation. The cell density used was 5×10^6/well. **(A)** The mRNA expression of TNF-α, IL-1β, iNOS, and PTGS2/COX-2 was quantitated in M1-stimulated macrophages. **(B)** The mRNA expression of MRC1/CD206, Chil3/Ym1, TGFβ1, and Arg1, was quantitated in M2-stimulated macrophages. *P < 0.05, **P < 0.01, ***P < 0.001, ****P < 0.0001. The data are expressed

as mean ± S.D.; n = 3 wells per group. **(C)** The levels of LXA_4 in the supernatant of BMDMs primed with LPS (100 ng/ml) or with IL-4/−13 (10 ng/ml). **(D)** The levels of MaR1 in the supernatant of BMDMs primed with LPS (100 ng/ml) or with IL-4/−13 (10 ng/ml). *P < 0.05, **P < 0.01, ***P < 0.001, ****P < 0.0001. The data are expressed as mean ± S.D.; n = 5 animals per group.